

Supplementary Information

Polymetallic sulfide assembly of $\text{Cu}_2\text{S}/\text{Ni}_3\text{S}_2$ grown in situ on Ni foam as a self-supported electrode and electrocatalyst for high-efficiency non-enzymatic glucose sensing

Jiahao Huang,^a Zichang Yang,^{b,c} Wu Li,^c Zhiyong Wang,^a and Chunxiang Zhu^{a,b*}

^aCollege of Design and Engineering, National University of Singapore, Singapore

117583, Singapore. E-mail: elezhucx@nus.edu.sg.

^bNational University of Singapore (Suzhou) Research Institute, Suzhou 215123, China.

^cCollege of Chemistry, Beijing Normal University, Beijing 100875, China.

1. Materials

Cu(NO₃)₂·3H₂O (Tianjin Damao Chemical Reagent Co., Ltd., 99.5%), thioacetamide (CH₃CSNH₂, Shanghai Macklin Biochemical Co., Ltd., 99.0%), potassium hydroxide (KOH, Xilong Scientific Co., Ltd, 85.0%), potassium chloride (KCl, Beijing Chemical Reagent Co., Ltd., 99.5%), sodium chloride (NaCl, Beijing Chemical Reagent Co., Ltd., 99.5%), D-glucose (C₆H₁₂O₆·H₂O, Xilong Scientific Co., Ltd), lactic acid (C₃H₆O₃, Shanghai Macklin Biochemical Co., Ltd., 85.5%~90%), uric acid (C₅H₄N₄O₃, Shanghai Macklin Biochemical Co., Ltd., 99%), L-alanine (C₃H₇NO₂, Shanghai Macklin Biochemical Co., Ltd., 99%), L-tyrosine (C₉H₁₁NO₃, Tianjin Bodie Chemical Co., Ltd). All the reagents were used without any further purification, except special instructions.

Nickel foam (NF) with thickness of 1.6 mm and density of 0.45 g·cm⁻³ was bought from Shenzhen Tianchenghe Technology Co., Ltd.), and required preprocessing before use. A large piece of NF was cut into many small pieces (area of 1×2 cm² each piece), which were then ultrasonically treated with 1 M HCl to remove the oxide layer. Subsequently, the NF pieces were ultrasonically treated in acetone, deionized water, and ethanol, followed by vacuum drying.

2. Electrochemical synthesis and measurements

The Cu/NF precursor was prepared via electrodepositing Cu⁰ metals on NF substrate under a CHI660 electrochemical workstation, using a three-electrode cell, with NF, graphite rod, and saturated calomel electrode (SCE) as working electrode, counter electrode, and reference electrode, respectively. All the electrochemical measurements were performed at this workstation. In this setup, the as-prepared NF-based materials acted as working electrode, platinum plate as counter electrode, and SCE as reference electrode.

3. Structural characterizations

The crystalline structures of the as-prepared samples were measured on a X pert pro MPD diffractometer (Cu K α radiation, $\lambda = 1.54056 \text{ \AA}$), operating at 40 kV and 40 mA. The morphologies of the as-prepared samples were examined by field emission scanning electronic microscope (SEM, SU-8010, Hitachi) at an acceleration voltage of

10 kV. Chemical states of the products were characterized by X-ray photoelectron spectroscopy (XPS) performed on an ESCALAB 250Xi spectrometer with Al K α radiation from Thermo Fisher.

Table S1. The simulated electrolyte resistance (R_e) and charge transfer resistance (R_{ct}) values based on the fitting models.

Samples	R_e (Ω)	R_{ct} (Ω)
Ni ₃ S ₂ /NF	4.17	30.31
Cu ₂ S/Ni ₃ S ₂ /NF-2	4.68	4.45
Cu ₂ S/Ni ₃ S ₂ /NF-4	4.48	2.76
Cu ₂ S/Ni ₃ S ₂ /NF-8	4.48	3.61

Table S2. Comparison of sensor performance in sensitivity, response time and limit of detection (LOD) at a signal/noise ratio of 3 by Cu₂S/Ni₃S₂/NF-4 at different voltages (0.40, 0.45, 0.50 and 0.50 V) and by different catalysts of Cu₂S/Ni₃S₂/NF-2 and Cu₂S/Ni₃S₂/NF-8 at 0.5 V.

Samples	Voltage (V)	Sensitivity (mA/mM ⁻¹ ·cm ⁻²)	LOD (μ M)	Response time (s)
Cu ₂ S/Ni ₃ S ₂ /NF-4	0.40	10.01	2.07	20
Cu ₂ S/Ni ₃ S ₂ /NF-4	0.45	18.33	0.64	20
Cu ₂ S/Ni ₃ S ₂ /NF-4	0.50	22.75	0.51	10
Cu ₂ S/Ni ₃ S ₂ /NF-4	0.55	18.86	1.93	10
Cu ₂ S/Ni ₃ S ₂ /NF-2	0.50	15.40	0.56	10
Cu ₂ S/Ni ₃ S ₂ /NF-8	0.50	16.91	0.63	10

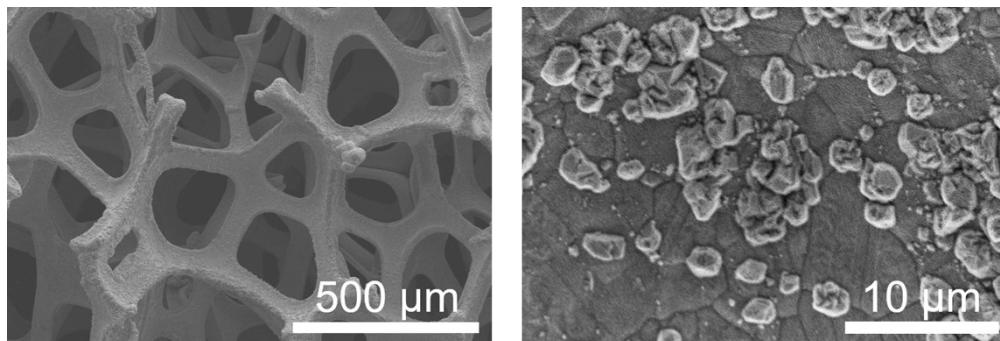


Fig. S1. SEM images of the Cu/NF precursor.

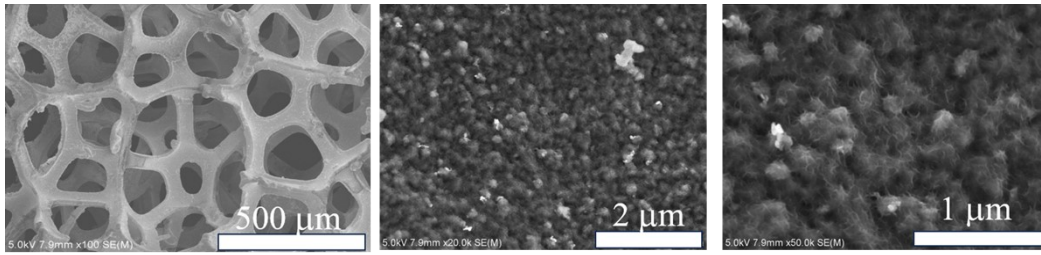


Fig. S2. SEM images of the control sample of $\text{Ni}_3\text{S}_2/\text{NF}$.

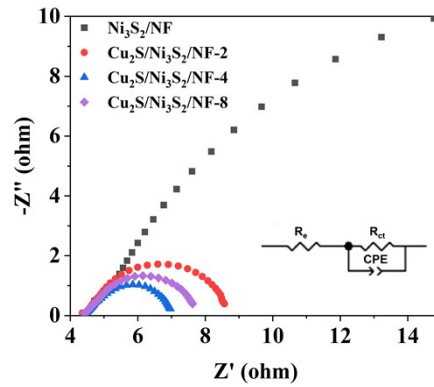


Fig. S3. Nyquist plots of EIS for the control sample of $\text{Ni}_3\text{S}_2/\text{NF}$ and composites of $\text{Cu}_2\text{S}/\text{Ni}_3\text{S}_2/\text{NF}-n$ ($n= 2, 4$ and 8).

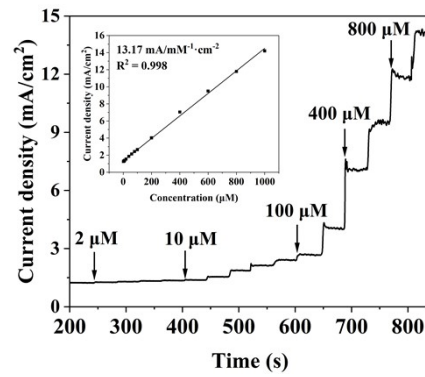


Fig. S4. Glucose oxidation chronoamperometry ($i-t$) of the control sample of $\text{Ni}_3\text{S}_2/\text{NF}$ at 0.5 V vs. SCE in 0.5 M KOH and the linear fit in response to glucose concentration.

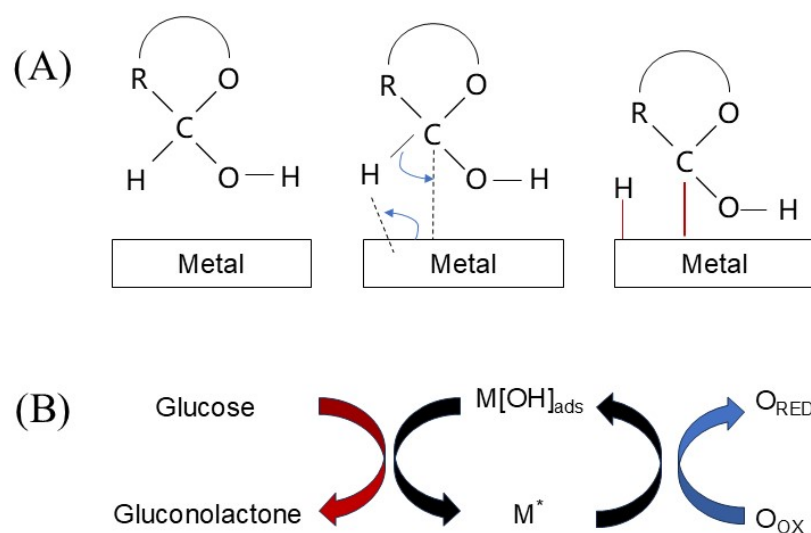


Fig. S5. (A) The steps of activated chemisorption model, (B) the incipient hydrous oxide adatom mediator (IHOAM) model. Redrawn based on the literature (*Biosens. Bioelectron.* 2020).¹

References

1. E. Schit and Z. Altintas, Significance of nanomaterials in electrochemical glucose sensors: An updated review (2016-2020), *Biosens. Bioelectron.*, 2020, **159**, 112165.